Title of Grant / Cooperative Agreement:	The role of Boundary Layer Clouds in the Global Energy and Water Cycle: An Integrated Assessment Using Satellite Observations
Type of Report:	Final Project Report
Name of Principal Investigator:	Ralf Bennartz
Period Covered by Report:	11/05/2012 - 11/04/2014
Name and Address of recipient's institution:	University of Wisconsin System, 21 N Park St Ste 6401, Madison, WI 53715-1218
NASA Grant / Cooperative Agreement Number:	NNX13AC05G

Reference 14 CFR § 1260.28 Patent Rights *(abbreviated below)*
The Recipient shall include a list of any Subject Inventions required to be disclosed during the preceding year in the performance report, technical report, or renewal proposal. A complete list (or a negative statement) for the entire award period shall be included in the summary of research.

Subject inventions include any new process, machine, manufacture, or composition of matter, including software, and improvements to, or new applications of, existing processes, machines, manufactures, and compositions of matter, including software.

Have any Subject Inventions / New Technology Items resulted from work performed under this Grant / Cooperative Agreement?	No ◉	Yes ○
If yes a complete listing should be provided here: Details can be provided in the body of the Summary of Research report.		

Reference 14 CFR § 1260.27 Equipment and Other Property (abbreviated below)
A Final Inventory Report of Federally Owned Property, including equipment where title was taken by the Government, will be submitted by the Recipient no later than 60 days after the expiration date of the grant. Negative responses for Final Inventory Reports are required.

Is there any Federally Owned Property, either Government Furnished or Grantee Acquired, in the custody of the Recipient?	No ◉	Yes ○
If yes please attach a complete listing including information as set forth at § 1260.134(f)(1).		

Attach the Summary of Research text behind this cover sheet.

Reference 14 CFR § 1260.22 Technical publications and reports (December 2003)
Reports shall be in the English language, informal in nature, and ordinarily not exceed three pages (not counting bibliographies, abstracts, and lists of other media).

A Summary of Research (or Educational Activity Report in the case of Education Grants) is due within 90 days after the expiration date of the grant, regardless of whether or not support is continued under another grant. This report shall be a comprehensive summary of significant accomplishments during the duration of the grant.

The role of boundary layer clouds in the global energy and water cycle: An integrated assessment using satellite observations

Final project report

November 2012 – November 2014

NASA Project Number: NNX13AC05G

Ralf Bennartz
Space Science and Engineering Center
University of Wisconsin – Madison

Table of Contents

1. Overview of accomplishments

1.1. Peer-reviewed publication with NEWS support

The following peer-reviewed publications were partly supported by NEWS-related activities

He, J., Y. Zhang, T. Glotfelty, R. He, R. Bennartz, J. Rausch, and K. Sartelet, 2015: Decadal Simulation and Comprehensive Evaluation of CESM/CAM5.1 with Advanced Chemistry, Aerosol Microphysics, and Aerosol-Cloud Interactions". Journal of Advances in Modeling Earth Systems, accepted.

Ban-Weiss, G. A., L. Jin, S. E. Bauer, R. Bennartz, X. Liu, K. Zhang, Y. Ming, H. Guo, and J. H. Jiang, 2014: Evaluating clouds, aerosols, and their interactions in three global climate models using satellite simulators and observations, J. Geophys. Res. Atmos., 119, doi:10.1002/ 2014JD021722.

Evan, A. T., R. J. Allen, R. Bennartz, and D. J. Vimont, 2013: The Modification of Sea Surface Temperature Anomaly Linear Damping Time Scales by Stratocumulus Clouds, J Climate, 26(11), 3619-363010.1175/jcli-d-12-00370.1.

1.2. Scientific studies in preparation

- Below are two short summaries of research accomplishments from this project since its inception in November 2012.
- Both studies are still in process of being refined so they can be submitted as peer-reviewed publications.
- Detailed results are provided in Section 2 of this report.

1.2.1. MODIS Collection 5 /6 comparison (R. Bennartz & J. Rausch (postdoc))

- MODIS data are key to characterizing cloud microphysics. NASA will soon provide a complete overhaul of their cloud retrievals (Termed 'Collection 6').
- In cooperation with NASA scientist S. Platnick and SSEC scientistB. Holz, we have assessed the impact of the improved retrievals on global cloud products.
- The results show significant differences between the two datasets with potentially significant impact on e.g. cloud Radiative forcing and the top-of-the-atmosphere energy balance.
- We are currently in the process of iteratively refining the results and summarizing them for peer-reviewed publication.

1.2.2. Regional studies: South-east Atlantic stratocumulus areas and biomass burning (R. Bennartz & E. Willmot (grad student))

- Regional study on the impact of biomass burning aerosol on cloud microphysics and reflectance was performed.
- It was shown that aerosol layers that touch the clouds lead to increased retrieved cloud droplet number concentration. For large aerosol optical depth, aerosols separated from the clouds might cause this effect too. The latter is an artifact caused by aerosol interacting radiatively with the cloud.
- In Year 2 we will further quantify aerosol effects, and their impact on albedo, which will ultimately lead to a refined assessment of the indirect aerosol effects.

2. Detailed Scientific Results

2.1. Comparison of Collection 5 and Collection 6 MODIS products

MODIS Collection 5 and 6 Cloud Product droplet effective radius retrievals at 1.6, 2.1 and 3.7 micron wavelengths and their corresponding cloud droplet number concentration values were aggregated and averaged upon a 1° x 1° grid over the period of 26 June – 3 August 2012. Cloud selection criteria consisted to warm

clouds (> 273K) over global oceans with valid effective radius and optical thickness retrievals over the latitudinal range of 45° S – 45° N. No retrieval quality assurance flags were applied to selection criteria. Additionally, values were calculated for pixels with valid retrievals common to both collections, hereafter referred to as Collections 5C and 6C.

Figure 1a and b show the spatial distribution of the 1.6 micron droplet radii from all valid retrievals respectively from Collections 5 and 6. Droplet radii from Collection 6 are greater than those of Collection 5 at all wavelengths by an average of 1.2 microns. Differences in the domain mean values of effective radii and their corresponding cloud droplet number concentrations are given in Table 1Table 2. This bias is likely attributable to Collection 6's retention of otherwise marginal retrievals that would normally be eliminated from Collection 5 by the Clear-Sky Restoral Algorithm. For pixels which are common to both collections, Collection 6C results are smaller at all wavelengths by approximately 0.4 – 0.5 micron which result in an increase in the calculated droplet number concentrations by approximately 10 cm-3. Whether these differences are solely attributable to differences in the retrieval algorithm or due to differences in quality assurance products will be the subject of further investigation.

Distributions of effective radii and CDNC for all valid pixels are given in Figure 2. The upper panels show the generally systematic shifts in effective radius between collections while the lower panels indicate the respective shifts in CDNC, whilst maintaining fairly similar distributions. For the common pixel panels in Figure 3, the droplet distributions are quit similar, with a slight shift to smaller radii and larger corresponding CDNC for Collection 6 retrievals.

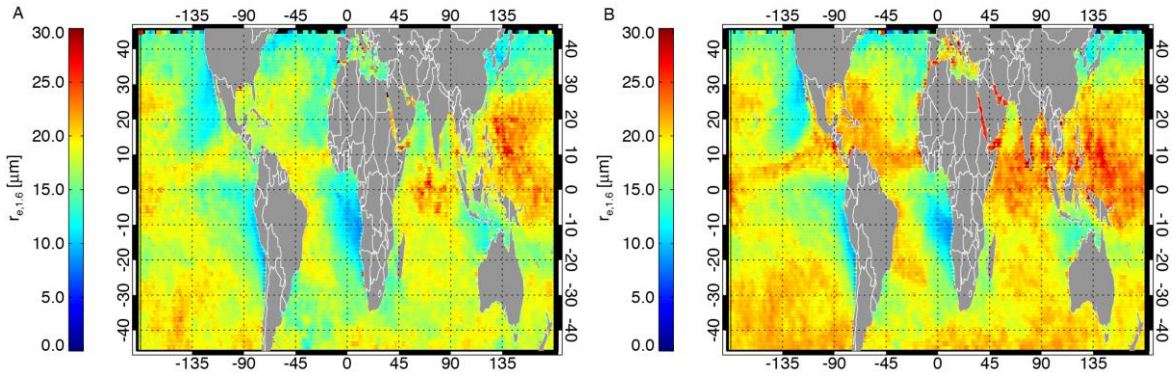

Figure 1. 1.6 micron retrievals of effective radius for a) Collection 5 and b) Collection 6.

Collection	Mean re,1.6	Median re,1.6	σ re,1.6	Mean re,2.1	Median re,2.1	σ re,2.1	Mean re,3.7	Median re,3.7	σ re,3.7

5	16.44	17.00	3.06	17.56	17.98	3.44	13.92	14.14	2.47
6	17.99	18.63	3.55	19.09	19.74	4.07	14.45	14.71	2.36
5C	16.30	16.92	2.90	16.42	16.75	3.06	13.74	13.96	2.45
6C	16.02	16.55	3.24	15.95	16.26	3.29	13.20	13.48	2.17

Table 1: Mean median and standard deviations (micron) of 1.6, 2.1 and 3.7 micron effective radius retrievals.

Collection	**Mean N1.6**	**Median N1.6**	**σ N1.6**	**Mean N2.1**	**Median N2.1**	**σ N2.1**	**Mean N3.7**	**Median N3.7**	**σ N3.7**
5	82.08	64.44	54.93	51.80	38.44	37.93	73.52	61.54	40.23
6	81.51	65.06	58.12	43.94	28.44	41.55	60.96	47.55	40.71
5C	82.18	64.72	54.96	56.80	43.73	38.44	77.62	65.36	42.29
6C	92.40	71.85	64.99	62.85	46.88	45.68	85.46	68.75	48.53

Table 2: Mean median and standard deviations (micron) of 1.6, 2.1 and 3.7 micron CDNC retrievals.

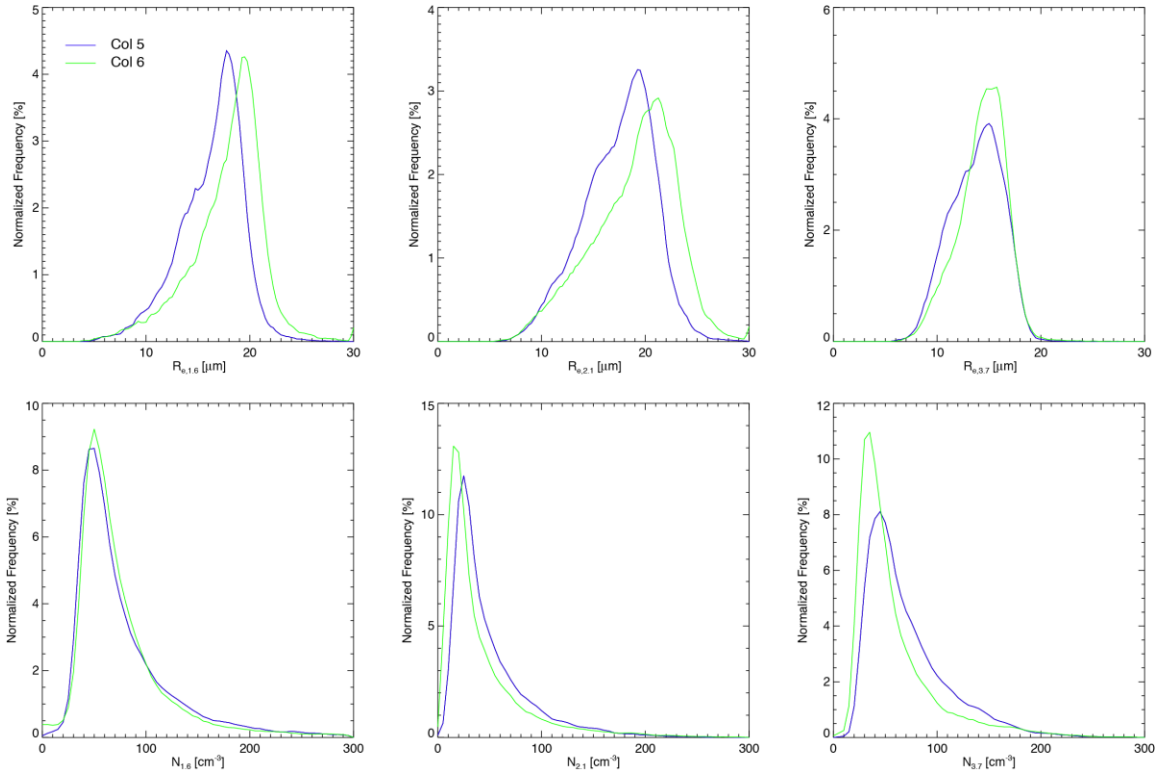

Figure 2: Histograms of Collection 5 and 6 retrievals of 1.6, 2.1 and 3.7 micron effective radius retrievals (upper panels) and CDNC (lower panels).

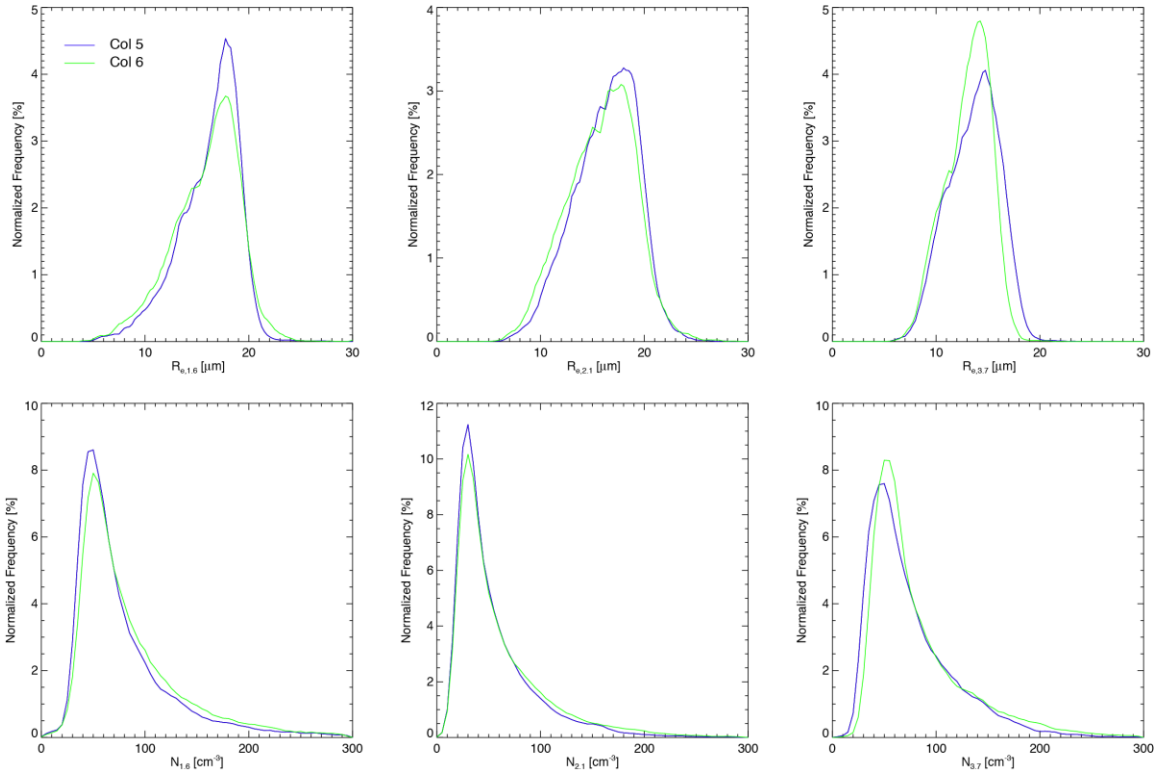

Figure 3: Same as Figure 2, but for Collection 5C and 6C retrievals.

2.2. Stratocumulus over the southeast Atlantic: Impact of biomass-burning aerosol on cloud optical properties and radiation balance

2.2.1. Abstract

The impact of overlying biomass-burning aerosols on cloud droplet number concentration and cloud effective radius of marine stratocumulus clouds in the South Atlantic Ocean is studied. Satellite data from the A-Train constellation from August 2006 to August 2007 were used to determine whether or not the layer of aerosols is detached from or touching the cloud. Using MODIS data and the 1064 nm backscatter profiles from the lidar aboard the Cloud-Aerosol Lidar and Infrared Pathfinder Satellite Observation (CALIPSO) satellite as opposed to the Cloud and Aerosol Layer products, which use the 532 nm backscatter profiles to detect cloud and aerosol features, yields a higher number of observations with aerosol layers touching the underlying stratocumulus cloud decks during peak biomass burning months. This is likely due to the fact that the 532 nm wavelength experiences more

attenuation from the aerosols and does not always correctly estimate the amount of aerosols close to the cloud top. Results show that for any given proxy aerosol optical depth, the cases where the aerosol layer touches the cloud will always yield a higher average cloud droplet number concentration and lower average droplet effective radius.

2.2.2. Introduction

Stratocumulus clouds cover vast areas of ocean, most often occurring in subtropical regions that experience strong subsidence. They can persist for long periods of time as they receive abundant moisture from oceans below which is then mixed throughout the layer via turbulence. In covering such a large area, these clouds will have an obvious effect on the Earth's radiation budget, and therefore the global climate, by reflecting and absorbing solar radiation. This effect can vary depending on cloud microphysical properties.

Anthropogenic air pollution adds aerosols into the atmosphere in large quantities. These aerosols act as cloud condensation nuclei upon which cloud droplets may form. It is well understood that clouds with high aerosol concentrations will contain more cloud drops at smaller sizes which can, in turn, reflect more sunlight back to space, thereby cooling the Earth [Twomey et al., 1984]. This effect is known as the first indirect aerosol effect and is currently one of the most uncertain forcings in our understanding of climate change [Forster and Ramaswamy, 2007].

In western Africa, significant amounts of vegetation are burned every year and mean easterly winds advect plumes of smoke and aerosols out over the South Atlantic Ocean where stratocumulus clouds are often located, thus the interaction between aerosols and clouds in this region is of particular interest. This study, focused on the region off the west coast of Africa, investigates the relationship between the aerosols produced by biomass burning and marine stratocumulus clouds.

Previous studies utilize the NASA Cloud-Aerosol Lidar and Infrared Pathfinder Satellite Observations (CALIPSO) Cloud and Aerosol Layer products to assess the vertical separation between biomass burning aerosol layers and low, liquid water clouds [[Devasthale and Thomas, 2011]; [Costantino and Breon, 2010]; [Wilcox, 2010]]. Devasthale and Thomas, (2011) show that there is a strong seasonality in events where biomass burning aerosols reside over low, liquid water clouds with the frequency of these events peaking in the September, October, and November months over the South Atlantic Ocean. They find that in 5-10% of all global overlap events (where aerosols reside over low liquid water clouds), the distance between the aerosol layer and the cloud is less than 100 m, while in 50% of the tropical overlap events the aerosols reside between 2 km and 4 km. Wilcox (2010) also uses the CALIPSO Cloud and Aerosol Layer products to show that the layer of aerosols produced by biomass burning in southern Africa usually resides between 2 km and 4 km as well, which is well above the stratocumulus decks that typically occur below

1.5 km. While this distinct separation of aerosols from the cloud has a significant impact on the radiative balance in this region, producing a net positive radiative forcing [Wilcox, 2012] and thus, a warming effect, it also suggests that the aerosols will have little effect on cloud microphysics. However, Bennartz (2007) and Costantino and Breon (2010) suggest that aerosols do play a role in changing cloud microphysics. This study uses an independent approach to determine if the aerosol layer does, in fact, affect cloud microphysics.

The CALIPSO Cloud and Aerosol Layer products used in the previously mentioned studies are determined using a threshold algorithm which inputs profiles of lidar attenuated scattering ratio data [Vaughan, 2005]. The wavelength of light used in these products falls within the visible spectrum and attenuates quickly due to scattering properties of aerosols and cloud droplets. This will tend to underestimate the amount of aerosols in the vicinity of the cloud (especially in instances of thick aerosol layers), thus creating a bias in the number of cases where aerosol layers touch the clouds. This study uses the lidar's longer, infrared wavelength backscatter profiles to determine whether or not aerosol layers touch the cloud, and what effect that will have on the cloud droplet number concentrations and droplet effective radii.

2.2.3. Datasets and Methods

For this study, data from the NASA A-Train satellite constellation were used; specifically, data from the Aqua-MODIS, CloudSat and CALIPSO satellites.

Aqua's Moderate Resolution Imaging Spectroradiometer (MODIS) instrument is a 36-band spectroradiometer that measures infrared and visible radiation at 1 km and 5 km spatial resolutions. The Level 2 narrow swath subset used in this study includes all MODIS data within 5 km of the CloudSat track. The 1 km data is used to derive cloud optical depth and a reference effective radius by combining observations at the 0.86 μm and 2.13 μm channels. The 5 km data is used to derive cloud top temperature as well as cloud fractional cover [Platnick et al., 2003].

The Cloud-Profiling Radar (CPR) aboard CloudSat is a 94-GHz radar that measures the power backscattered by clouds at a 500 m vertical resolution. A vertical profile is generated approximately every 1.1 km along the track with a vertical sampling of 250 m. The Level 1B CPR data is used to determine information about cloud top heights as well as latitude, longitude, and time of overpass [Stephens et al., 2002].

The Cloud-Aerosol Lidar with Orthogonal Polarization (CALIOP) is a two-wavelength lidar aboard CALIPSO that produces high-resolution vertical profiles of clouds. CALIOP measures backscatter intensities at 1064 nm and 532 nm as well as the perpendicular attenuated backscatter at 532 nm. The vertical resolution ranges from 30 m to 60 m. Level 1B data contains the three aforementioned backscatter profiles. The Level 2 Cloud Layer product contains integrated attenuated backscatter and cloud optical depth on a 5 km horizontal grid. The Level 2 data also includes a vertical feature mask that describes the vertical and horizontal distribution of cloud and aerosol layers based on the 532 nm backscatter profiles.

Data from the A-Train satellites were selected for the region of interest: 5.0°S to 30.0°S and 10°W to 15°E off the west coast of Africa where stratocumulus clouds are often observed. The data were filtered to include only daytime observations where cloud top temperatures, measured from Aqua's MODIS instrument, exceed 273 K (warm clouds). The data were further filtered to include only observations where the cloud top height, measured by the CPR and CALIOP, falls between 0.3 km and 2.5 km.

Aerosol optical thickness was calculated by multiplying CALIOP's optical depth measurements (both 532 nm and 1064 nm wavelengths) by biomass burning lidar ratios as determined by CALIOP's Algorithm Theoretical Basis Document [Liu, 2005]. For 532 nm, the assumed lidar ratio was chosen to be 65 and for 1064 nm, the assumed lidar ratio was 31. In order to correct for lidar noise during the daytime, a constant offset was subtracted to create a proxy aerosol optical thickness.

The data was sorted into four bins as shown in Table 1. The difference between CALIOP and CPR's cloud top height measurements is labeled |CTHCPR-CTHCALIOP|. If this difference exceeds 1 km, it was placed in a bin of rejected data. MODIS's cloud optical depth measurement is labeled CODMODIS. If this value is less than 0.1, it was also placed in the rejection bin. To determine whether or not the aerosol layer touches the cloud, the change in aerosol optical depth in a 300 m layer above the cloud is determined using the 1064 nm optical depth measurements from CALIOP (ΔAOD1064). The 1064 nm is less noisy and will help minimize any adverse effects of attenuation, which frequently occurs at 532 nm. The thresholds shown in Table 1 have been set after visually inspecting multiple vertical profiles.

In order to compare the microphysical differences between clouds with higher aerosol concentrations to those with smaller aerosol concentrations, cloud droplet number concentration and a proxy aerosol optical depth are calculated and compared. As we are most interested in the interaction between the aerosol layer and the cloud top, we calculated a proxy aerosol optical depth using the 1064 nm and 532 nm aerosol optical thicknesses calculated previously. The cloud top height was determined by the lowest altitude at which the 532 nm total attenuated backscatter exceeded 0.015 km-1sr-1. This threshold was set after visually inspecting multiple vertical profiles of total attenuated backscatter to determine at which value the lidar typically registers the cloud top. Adding 90 m to this value ensures we are definitely above the cloud top. The vertically-integrated optical thicknesses previously calculated at this height (cloud top height plus 90 m) are used as the proxy aerosol optical depth and will be labeled as PAOD. The 1064 nm PAOD is used for the remainder of this study in order to minimize adverse effects of attenuation.

Cloud Droplet Number Concentration, N, is calculated using MODIS observations, specifically cloud optical thickness (τ), droplet effective radius (reff), cloud fraction (CF), and cloud top temperature. Bennartz (2007) derives the following equation, which has been used in this study:

$$N = \frac{2^{-5/2}}{k} t^{3} \left[\frac{W}{C_F}\right]^{-5/2} \left[\frac{3}{5} \rho Q\right]^{-3} \left[\frac{3}{4 \rho r_L}\right]^{-2} c_w^{1/2} \quad (0.1)$$

where liquid water path, W, is calculated using the assumption of an adiabatically stratified cloud.

$$W = \frac{5}{9} r_L t r_{eff} \quad (0.2)$$

The ratio between the volume mean radius and effective radius, k, is assumed to be a constant 0.8 [Martin et al., 1994], and scattering efficiency, Q, is assumed to be 2. The condensation rate, cw, is calculated in kg m-4 from the MODIS cloud top temperature observations. The clouds are assumed to be at 80% of their adiabatic value, and thus, cw is multiplied by 0.8.

2.2.4. Results

Cloud Microphysics

Data from August 2006 to August 2007 were analyzed. A total of 2,957 vertical profiles had aerosol layers touching the cloud, and 2,451 profiles had aerosol layers separated from the cloud. All other data were rejected or put into the uncertain bin (see Fig. 1). The biomass burning months (June through September) are characterized by high numbers of cases where the aerosol layer touches the cloud compared to cases where the aerosol layer does not touch the cloud. In the remaining months, there are more cases where the aerosol layer does not touch the cloud compared to cases where it does touch the cloud. Data placed in the rejection bin may be due to large differences in cloud top height measurements between CPR and CALIOP, or the presence of overlying ice clouds.

There is an obvious effect on cloud droplet number concentration and droplet effective radius when aerosols interact with the clouds regardless of PAOD value (Fig. 2). This is seen in comparing PAOD to cloud droplet number concentration and effective radius for cases where the aerosol layer touches the cloud and cases where it does not touch the cloud. Cases where the aerosol layer interacts with the cloud show higher concentrations of cloud droplets, with an average N of 107.98 ± 63.783 cm-3. When the aerosol layer is detached from the cloud, there are fewer cloud droplets with an average N of 57.04 ± 39.734 cm-3. Regardless of PAOD, the droplet

effective radius is smaller when the aerosol layer interacts with the cloud, with an average reff of 13.355 ± 3.590 μm. The droplet effective radius is larger when aerosols are detached from the cloud, with an average reff of 16.374 ± 4.269 μm. Table 2 summarizes the mean and median values of PAOD, N, and reff for both cases.

The standard MODIS retrievals of optical depth and effective radius over oceans are calculated using the 0.86 μm non-absorbing band in combination with the 2.13 μm band. Previous studies on the retrieval accuracy of such parameters have shown that there is a systematic low bias in the cloud optical depth in the presence of overlying partially-absorbing aerosols due to the increased absorption within the aerosol layer, thereby decreasing the 0.86 μm radiances [[Wilcox et al., 2009]; [Haywood et al., 2004]]. This reduction in cloud optical depth leads to an underestimate of cloud droplet number concentration [Bennartz and Harshvardhan, 2007]. However, Haywood et al., [2004] find that the effect of including overlying aerosols on retrievals of effective radius with these two bands is small, and does not exceed 1 μm.

Comparison of 532 and 1064 nm Wavelengths

The method used by Devasthale and Thomas (2011) to determine the vertical separation of an aerosol layer and stratocumulus cloud layer was compared against our method in order to investigate the differences between using the 532 nm and 1064 nm. Devasthale and Thomas (2011) use the CALIOP Vertical Feature Mask to find profiles where there is an aerosol flag and a liquid water cloud flag within the same vertical column, both of which are of the highest confidence. An aerosol layer and cloud layer are considered touching by this method if the distance between the lowest level of the aerosol layer and the highest layer of cloud is less than 100 m. From August 2006 to August 2007, this process yields a total of 9,071 vertical profiles. Applying our method to these profiles produces the results shown in Table 3. Our method results in a greater number of profiles where aerosol layers touch the cloud during the peak biomass burning months compared to the Devasthale and Thomas (2011) method. The most significant difference can be seen in the month of August 2007, where Devasthale and Thomas (2011) would constitute 172 profiles as having aerosol and cloud layers interacting, and our method finds 1,030 of such profiles (Fig 3). However, during the non-peak biomass burning months (October – May), the Devasthale and Thomas (2011) method results in greater numbers of profiles where aerosol layers touch the cloud.

Conclusions

We present an independent approach using data from the A-Train satellites to investigate the vertical separation of biomass burning aerosol and marine stratocumulus cloud layers and to what extent their interaction affects cloud microphysics. The area of study focuses off the west coast of Africa over the South

Atlantic Ocean from August 2006 to August 2007. In this region, biomass burning injects plumes of aerosols into the atmosphere that are transported over the ocean where large, persistent stratocumulus cloud decks often occur. It is well understood that aerosols residing above low, liquid water clouds will change the radiative effect of those clouds, but it is not well understood at what magnitude. The impact of aerosols on cloud microphysics further complicates this issue. The goals of this study include: (1) determining when aerosols interact with the cloud decks, (2) what effect this interaction has on cloud microphysics, specifically cloud droplet number concentration and droplet effective radius, and (3) determining if the lidar wavelength used to calculate the above processes affects the outcome.

This study demonstrates that at any proxy aerosol optical depth (calculated by vertically integrating optical thicknesses), cases where the aerosol layer touches the cloud will always yield a higher average cloud droplet number concentration and lower average droplet effective radius than cases where the aerosol layer is separated from the cloud. This suggests that interactions between aerosol and cloud layers have a significant impact on cloud microphysics and it is more than a retrieval artifact of the satellite data. This effect on cloud microphysics, in turn, will alter the net radiative effect.

Similar to other studies [e.g. [Devasthale and Thomas, 2011]], this study shows that cases where aerosols interact with the underlying clouds are not negligible, however, we believe the number of these cases is being underestimated. Previous studies [e.g. [Devasthale and Thomas, 2011]; [Wilcox, 2010]] use the CALIPSO Cloud and Aerosol Layer Products, which use the lidar's 532 nm wavelength to determine when aerosols and clouds interact. This study uses the longer, 1064 nm wavelength to determine, quantitatively, when these layers interact in hopes of minimizing the adverse affects of attenuation caused by absorbing aerosols. Results show that the number of these cases occurring during the peak biomass burning months (June – September) is in fact, underestimated, while during the biomass burning offseason (October – May), the number is overestimated.

Further investigation is needed to understand and quantify the various direct and indirect effects the aerosols can induce on the clouds, and on a global scale.

Tables

Table 1. Thresholds determining which bin each vertical profile belongs to

Bin	$\lvert CTH_{CPR}-CTH_{CALIOP}\rvert$	COD_{MODIS}	ΔAOD_{1064}
Aerosol Layer Touches Cloud	$\leq$ 1 km	$\geq$ 0.1	> 0.025
Aerosol Layer Does Not Touch Cloud	$\leq$ 1 km	$\geq$ 0.1	< 0.005
Uncertain if Aerosol Layer touches cloud	$\leq$ 1 km	$\geq$ 0.1	0.025 < ΔAOD < 0.005
Rejections	> 1 km	< 0.1	N/A

Table 2. Mean and Median Proxy Aerosol Optical Depth, N, and Droplet Effective Radius statistics for both cases

Case	Total # of Observations	Mean PAOD	Median PAOD	Mean N [cm^{-3}]	Median N [cm^{-3}]	Mean r_{eff} [μm]	Median r_{eff} [μm]
Aerosol Touches Cloud	2,957	0.475 ± 0.100	0.466	107.982 ± 63.783	96.368	13.355 ± 3.590	12.845
Aerosol Does Not Touch Cloud	2,451	0.331 ± 0.066	0.322	57.041 ± 39.734	50.414	16.374 ± 4.269	15.453

Figures

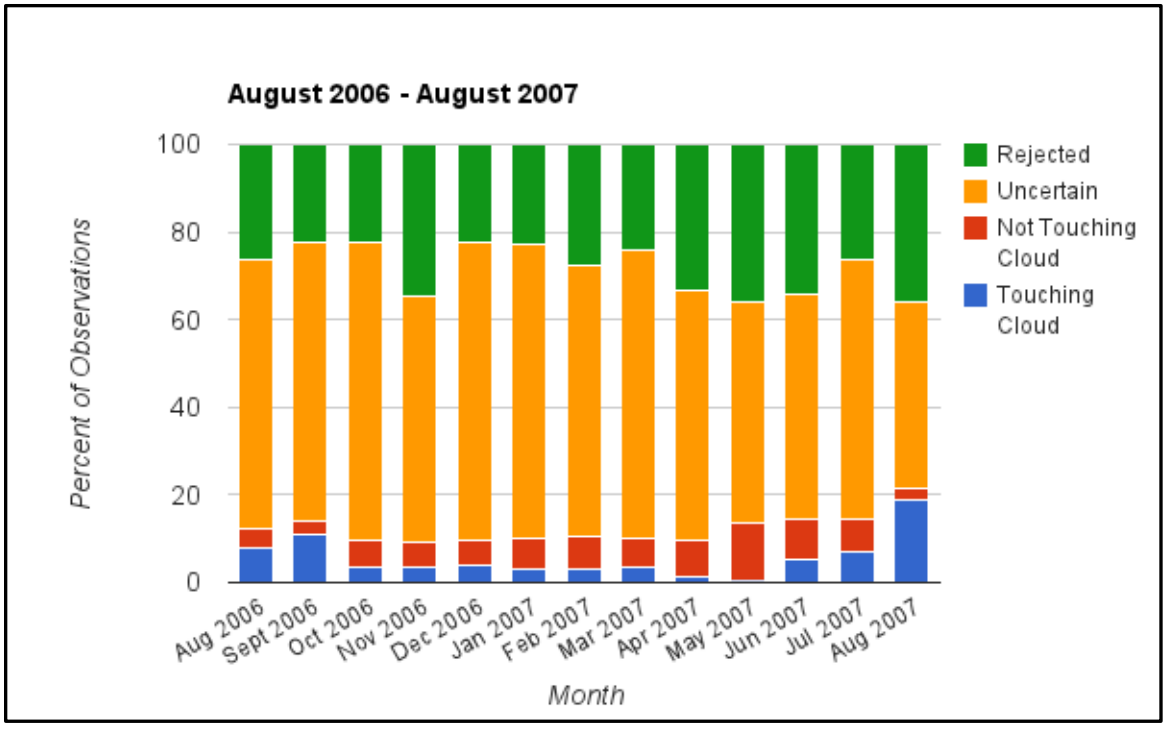

Figure 4: Percentage of observations each month from August 2006 to August 2007. Blue is percentage of cases where aerosol layers touch the cloud, red is percentage of cases where aerosol layers do not touch the cloud, orange is percentage of cases where aerosol layers touching the cloud is uncertain, and green is all rejected data.

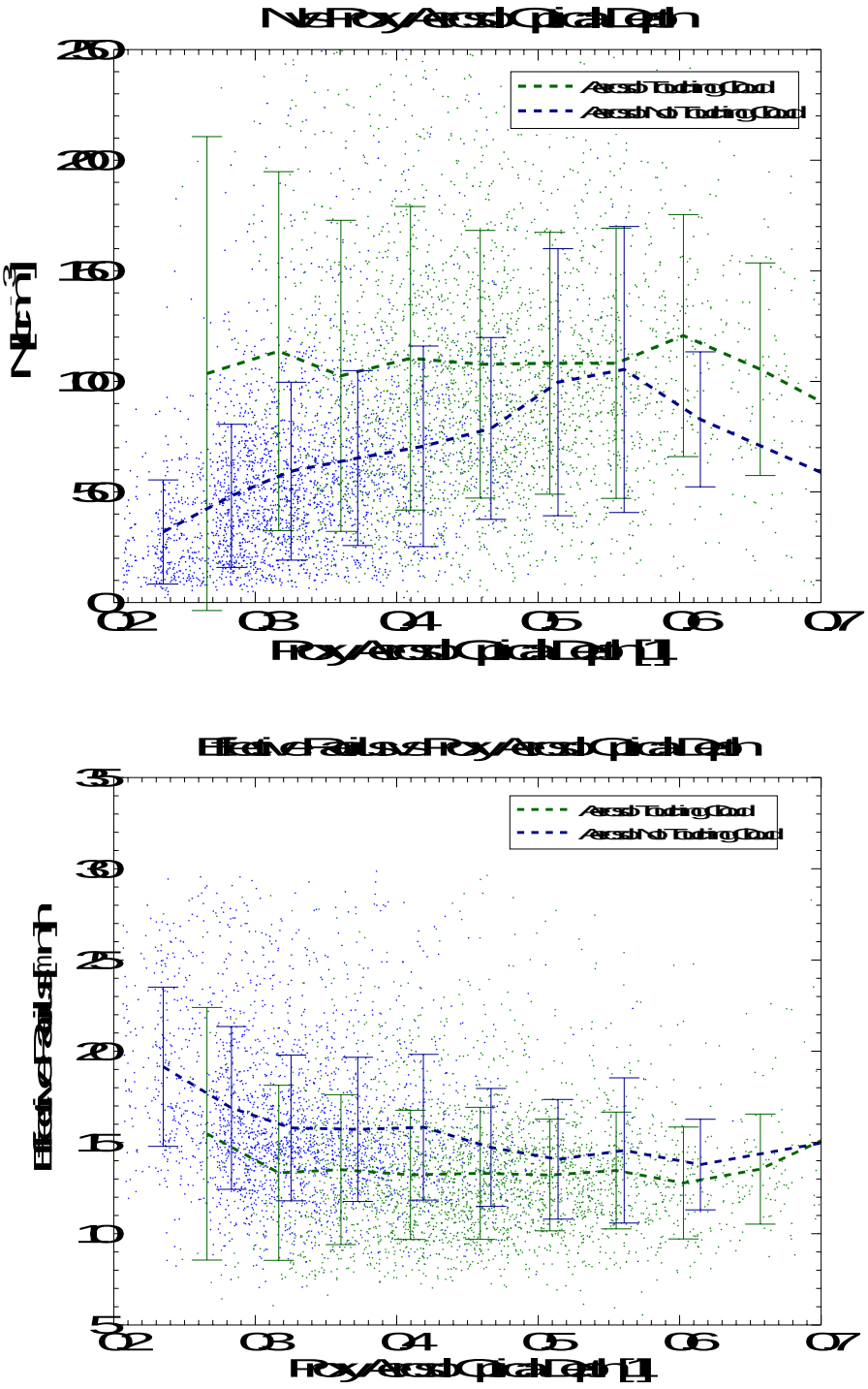

Figure 5: Top: PAOD vs Cloud Droplet Number Concentration [cm^{-3}] for cases where aerosol layers touch the cloud (green) and cases where the aerosol layer does not touch the cloud (blue). Bottom: PAOD vs droplet effective radius [μm] for cases where aerosol layers touch the cloud (green) and cases where the aerosol layer does not touch the cloud (blue).

3. References

Bennartz, R., and Harshvardhan (2007), Global assessment of marine boundary layer cloud droplet number concentration from satellite (vol 112, artn no. D02201, 2007), J Geophys Res-Atmos, 112(D18)Artn D16302, Doi 10.1029/2007jd008841.

Costantino, L., and F. M. Breon (2010), Analysis of aerosol-cloud interaction from multi-sensor satellite observations, Geophys Res Lett, 37Artn L11801, Doi 10.1029/2009gl041828.

Devasthale, A., and M. A. Thomas (2011), A global survey of aerosol-liquid water cloud overlap based on four years of CALIPSO-CALIOP data, Atmos Chem Phys, 11(3), 1143-1154Doi 10.5194/Acp-11-1143-2011.

Forster, P., and V. Ramaswamy (2007), Changes in Atmospheric Constituents and in Radiative Forcing, Climate Change 2007: The Physical Science Basis, 129-234

Haywood, J. M., S. R. Osborne, and S. J. Abel (2004), The effect of overlying absorbing aerosol layers on remote sensing retrievals of cloud effective radius and cloud optical depth, Q J Roy Meteor Soc, 130(598), 779-800

Liu, Z. O., A.;Hu, Y.;Vaughan, M.;Winker, D. (2005), CALIOP algorithm theoretical basis document -- Part 3: Scene classification algorithms

Martin, G. M., D. W. Johnson, and A. Spice (1994), The Measurement and Parameterization of Effective Radius of Droplets in Warm Stratocumulus Clouds, J Atmos Sci, 51(13), 1823-1842

Platnick, S., M. D. King, S. A. Ackerman, W. P. Menzel, B. A. Baum, J. C. Riedi, and R. A. Frey (2003), The MODIS cloud products: Algorithms and examples from Terra, Ieee T Geosci Remote, 41(2), 459-473Doi 10.1109/Tgrs.2002.808301.

Stephens, G. L., et al. (2002), The cloudsat mission and the a-train - A new dimension of space-based observations of clouds and precipitation, B Am Meteorol Soc, 83(12), 1771-1790Doi 10.1175/Bams-83-12-1771.

Twomey, S. A., M. Piepgrass, and T. L. Wolfe (1984), An Assessment of the Impact of Pollution on Global Cloud Albedo, Tellus B, 36(5), 356-366

Vaughan, M. A. W., D. M.; Powell, K. A. (2005), CALIOP Algorithm Theoretical Basis Document Part 2: Feature Detection and Layer Properties Algorithms(Release 1.01)

Wilcox, E. M. (2010), Stratocumulus cloud thickening beneath layers of absorbing smoke aerosol, Atmos Chem Phys, 10(23), 11769-11777Doi 10.5194/Acp-10-11769-2010.

Wilcox, E. M. (2012), Direct and semi-direct radiative forcing of smoke aerosols over clouds, Atmos Chem Phys, 12(1), 139-149Doi 10.5194/Acp-12-139-2012.

Wilcox, E. M., Harshvardhan, and S. Platnick (2009), Estimate of the impact of absorbing aerosol over cloud on the MODIS retrievals of cloud optical thickness and effective radius using two independent retrievals of liquid water path, J Geophys Res-Atmos, 114Artn D05210, Doi 10.1029/2008jd010589.